NANO MICRO small

Selective Detection of Target Proteins by Peptide-Enabled Graphene Biosensor

*Dmitriy Khatayevich, Tamon Page, Carolyn Gresswell, Yuhei Hayamizu, William Grady, and Mehmet Sarikaya**

Direct molecular detection of biomarkers is a promising approach for diagnosis and monitoring of numerous diseases, as well as a cornerstone of modern molecular medicine and drug discovery. Currently, clinical applications of biomarkers are limited by the sensitivity, complexity and low selectivity of available indirect detection methods. Electronic 1D and 2D nano-materials such as carbon nanotubes and graphene, respectively, offer unique advantages as sensing substrates for simple, fast and ultrasensitive detection of biomolecular binding. Versatile methods, however, have yet to be developed for simultaneous functionalization and passivation of the sensor surface to allow for enhanced detection and selectivity of the device. Herein, we demonstrate selective detection of a model protein against a background of serum protein using a graphene sensor functionalized via self-assembling multifunctional short peptides. The two peptides are engineered to bind to graphene and undergo co-assembly in the form of an ordered monomolecular film on the substrate. While the probe peptide displays the bioactive molecule, the passivating peptide prevents non-specific protein adsorption onto the device surface, ensuring target selectivity. In particular, we demonstrate a graphene field effect transistor (gFET) biosensor which can detect streptavidin against a background of serum bovine albumin at less than 50 ng/ml. Our nano-sensor design, allows us to restore the graphene surface and utilize each sensor in multiple experiments. The peptide-enabled gFET device has great potential to address a variety of bio-sensing problems, such as studying ligand-receptor interactions, or detection of biomarkers in a clinical setting.

1. Introduction

Detection of molecular recognition events ex situ has been a well-established approach to drug discovery and molecular biology research since the 1960s.[1] More recently, it has been applied in clinical research and practice for diagnosing and monitoring diseases, including several types of cancer, through the detection of biomarkers in blood, tissues, or urine of a patient.[2] Among the techniques used to detect such markers are the surface plasmon resonance spectroscopy (SPR),[3,4] quartz crystal microbalance (QCM),[5] various immunoassays including electrochemical assays and others.[6–9] The applicability of these techniques to clinical practice remains limited, however, since the markers are present in very low concentrations against a background of high abundance serum or tissue proteins, requiring high selection efficiency of the sensor. During the last several years,

D. Khatayevich, T. Page, C. Gresswell,
Prof. M. Sarikaya
GEMSEC, Genetically Engineered Materials Science and Engineering Center
Materials Science and Engineering
University of Washington
302 Roberts Hall, Seattle, WA 98195, USA
E-mail: sarikaya@u.washington.edu
Prof. Y. Hayamizu
Polymer Science and Technology
Tokyo Institute of Technology
Ookayama, Japan
Prof. W. M. Grady
Fred Hutchinson Cancer Research Center
Seattle, WA 98109, USA

DOI: 10.1002/smll.201302188

two-dimensional single layer material-based field effect transistor (2D-FET) (such as graphene) sensors have been employed for ultrasensitive detection of molecules.[10–14] Graphene and 1-D carbon nano-tubes in particular have been used successfully to achieve a very low detection limit,[15–21] with designs reported to detect femtogram per milliliter concentrations of analyte.[22] These levels of sensitivity is possible due to the excellent electronic properties of graphene, resulting from delocalized π-bond structure, and zero band gap, which is highly sensitive to molecular doping.[23–26] Charge transfer and Hall doping, resulting from the interactions of molecules with the graphene, the sensor material, change its Dirac point and, therefore, its resistance.[12,22,27] When a molecule, such as a protein, adsorbs to or is specifically captured by the graphene sensor, the change in resistance could allow specific detection of the event at the molecular level. Based on this proposition, and to establish a highly sensitive 2D-FET biosensor, target-specific bioprobes must be immobilized onto the sensor's surface in a controlled manner with a simple process while preserving the functionality of the sensor substrate.

A number of graphene functionalization routes have been employed so far involve covalent bonding, e.g., via the introduction of carboxylic groups, so as to control the interface with graphitic materials.[28–30] To preserve the intrinsic properties of graphene, methods of non-covalent functionalization via π–π stacking using aromatic chemistry have also been used.[31–33] In order to enhance probe density on the surface pre-functionalized nano-particles, for example, gold, have been adsorbed to graphene sensors resulting in high sensitivity biosensors.[34,35] In addition to these successful chemical and physicochemical functionalization techniques, non-invasive approaches using peptides have been demonstrated as a biocompatible alternative to controlling the surface properties of graphitic materials. Selected using combinatorial peptide libraries, these engineered solid-binding peptides offer a versatile platform for bridging the bio/inorganic divide.[36–38] These short (7–14 amino acids long) peptides have strong-binding capability (k_d = 50 nM to 1 μM), exhibit a wealth of chemical diversity, and are materials specific. The solid-binding peptides have a modular capacity which allows the control of functional diversity through simple point and domain mutations and targeted chemical modification, providing unique opportunities to control binding, chemical properties, and biofunctional display.[39,40] Instead of covalent bonding prevalent among the synthetic linkers (e.g., thiols and silanes), these short peptides, due to their specific folding patterns on surfaces dictated by their sequences, bind to solids through weak intermolecular forces at multiple positions at the peptide/solid interface. This enables the solid binding peptides to assemble and function in aqueous solutions and in biological buffers.[41–43] Various graphite,[44] graphene-,[45–47] and CNT-binding[48,49] peptide sequences and poly amino acids have been identified in the literature through combinatorial display and other means. They have been employed for applications such as bioinorganic nano-material formation,[50] and non-specific control of surface chemistry.[44] The dodecapeptide GrBP5-WT (with amino acid sequence: IMVTESSDYSSY, affinity constant: K_a = 3.78 μM^{-1}) is unique among graphite- and CNT-binding peptide sequences identified so far as, upon binding, it forms long-range ordered, uniform, and crystallographic molecular nanostructures on graphitic materials. Furthermore, it has been demonstrated in this research group,[51] that the peptide nanostructures can be controlled through sequence mutation that allows to tune intermolecular and peptide-substrate interactions (**Figure 1**). Having a modular structure, the wild-type (GrBP5-WT) peptide can be designed to expose predictable surface chemistry through the display of specific amino acids, making it ideal for presenting molecular probes, ligands, anti-bodies, and other sensing molecules in a controllable fashion (Figure 1A). Moreover, it has been shown that two mutants of GrBP5-WT can be simultaneously assembled to display a combination of properties on the graphitic substrate.[52] Multi-functionality is critical to the application of a biomarker sensor in clinical practice, since in addition to possessing sensitivity, it must be capable of discriminating for the target against a background of proteins present in the sample. It is, therefore, essential to simultaneously impart targeting and anti-fouling capabilities to the sensor.

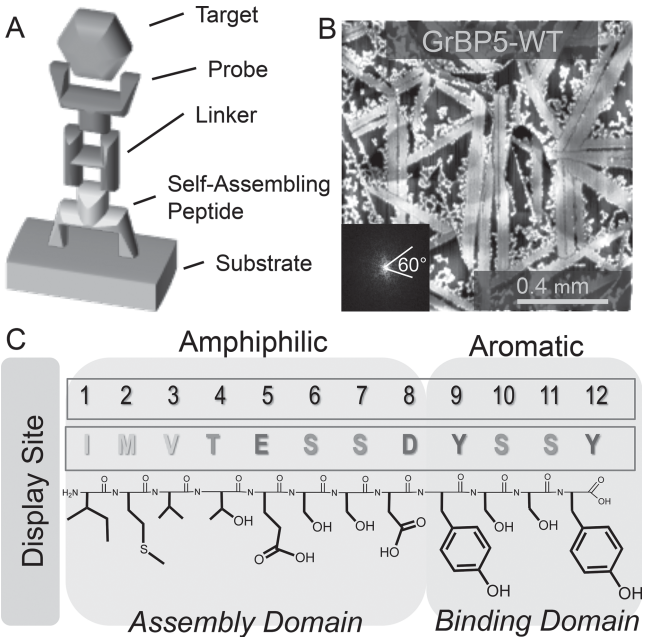

Figure 1. A) Conceptual schematics of the modular peptide based approach for biosensor functionalization; B) AFM image showing the formation of GrBP5-WT monomolecular ordered film on graphite. Inset is a fast Fourier transform of the image showing hexagonal ordering of the WT peptide on graphite crystal surface lattice. C) The amino acid sequence of WT-GrBP5 showing the primary domains with different biochemical/physical functionalities.

In the present study, we demonstrate selective detection of a model protein against a background of an abundant serum protein using a graphene biosensor functionalized via two types of co-assembled, multifunctional, self-assembling peptides which simultaneously display the probe and also prevent non-specific adsorption. In particular, we employ a 4-probe graphene field effect transistor (gFET) sensor (**Figure 2**), functionalized using co-assembled mutants of GrBP5-WT, displaying biotin, and SS-GrBP5 mutant, hydrophilic residues at the N-terminus (**Table 1**), to detect

NANO MICRO small

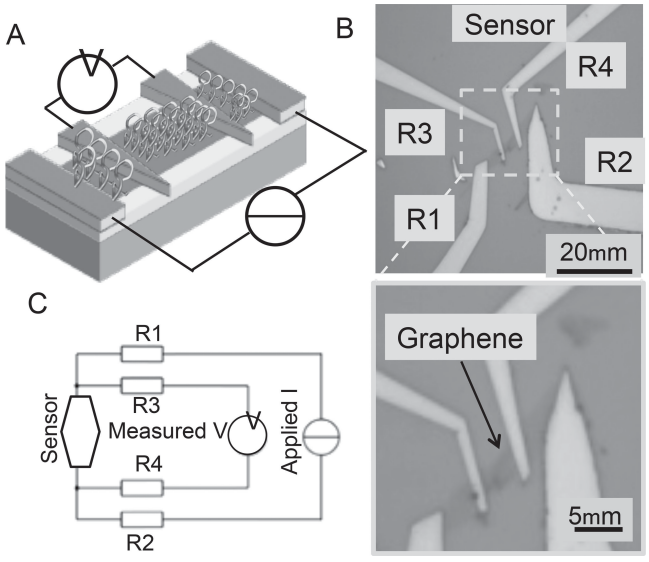

Figure 2. A) Schematic illustration of the four-probe bio-functionalized graphene field effect transistor with self-assembled peptides; B) Optical microscopy image of the sensor device at two different magnifications; C) Equivalent electrical circuit of the gFET device.

streptavidin (SA) against a background of bovine serum albumin (BSA). Furthermore, a regeneration protocol has also been developed which allows one to utilize a single sensor for over 12 experiments. Through this study, we establish a methodology for single-step bio-functionalization of graphitic sensors and show its performance and sensitivity for the detection of biomolecules at low concentrations. The proof-of-principle demonstration of the peptide-enabled graphene FET biosensor herein can be applied to a variety of analytes in complex solutions.

2. Results and Discussion

2.1. Graphene Biosensor

The graphene biosensor was fabricated using electron beam lithography in a four probe configuration (Figure 2). Such configuration is advantageous, because it minimizes the effect of contact resistance on the measurement, increasing the signal to noise ratio. This is accomplished by supplying a constant current via contacts R1 and R2, and monitoring the voltage between the contacts R3 and R4 at negligible currents (Figure 1C).

In order to test the capabilities of the graphene field effect transistor sensor, as well as to ensure that our peptide-based functionalization scheme appropriately displays the probe, we created a biotin-graphite binding peptide (bio-GrBP5) fusion molecule (Table 1). By sequential introduction of increasing concentrations of the bi-functional peptide to the sensor, we were able to determine the ultimate sensitivity of our system, and to create a dense, uniform monolayer of self-assembled biotinylated peptide (**Figure 3**A, C). We then introduced streptavidin (SA) to the system in sequentially increasing concentrations to determine if the sensitivity significantly diminishes with distance from the sensor. The AFM images (Figure 3B), along with the sensogram (Figure 3C) demonstrate binding of streptavidin to the biotinilated sensor surface. The height difference of about 2 nm is observed between the peptide only and that with the SA added surfaces. Moreover using the three-sigma method, based on an average of multiple sensor measurements, we calculated the detection limit of our device to be 30 µg/ml (+/- 7 µg/ml), for both the bare and the functionalized surface. The differences in morphology in the two AFM images indicate that there is a certain amount of instability introduced into the peptide by the analyte; however, the coverage

Table 1. Molecular Characteristics of the Designed Peptides.

Molecule	Sequence[a)]	Mol. Mass	G.R.A.V.Y.[b)]
GrBP5-WT	IMVTESSDYSSY	1381.4	−0.242
Bio-GrBP5	bio-IMVTESSDYSSY	1624.3	0.185
SS-GrBP5	SS-IMVTESSDYSSY	1555.6	−0.321
Bio-SS-GrBP5	bio-SS-IMVTESSDYSSY	1798.5	0.264

[a)]Residues colored by properties: Non-polar – orange; Polar – green; Charged – red; Aromatic – brown; [b)]Grand average hydropathy index.

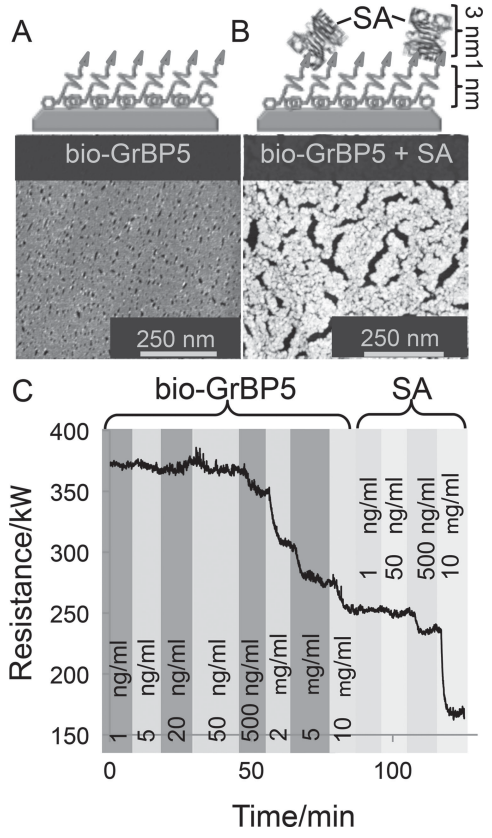

Figure 3. A) AFM image and schematics of 10 mg/ml bio-GrBP5 self-assembled on graphite; B) AFM image and schematics of 10 mg/ml streptavidin captured by the bio-GrBP5 monolayer; C) Corresponding sensogram of sequential addition of increased concentrations of bio-GrBP5 followed by the sequential addition of increased concentrations of streptavidin (SA).

remains above 85% after two hours of testing, which is well beyond the time required to achieve apparent binding equilibrium. As a control, we also tested the binding of SA to the un-functionalized sensor, finding that no detectable binding occurs in the range of concentrations used (Figure S1 in supplementary information).

Even a few layers of adsorbed water molecules provide sufficient dielectric screening of the charged impurities to prevent their affect as scatterers on the carriers in graphene while allowing them to be dopants.[53] In our case, the FET is embedded in water, and the peptides adsorbed on the surface cause doping through the probe-target interaction affecting a shift in the overall resistance of graphene-FET. The response of our sensor is consistent with those reported previously for graphene-based biosensors.[16,54] The decrease in resistance in the presence of the biomolecule is explainable through increased doping of the graphene layer by ionic and partial charges of the peptidic molecules. The sign of the resistance change is dependent on the gating conditions of the gFET, which are not controlled in the present device. The change in resistance can, therefore, be treated as arbitrary intensity units for the purposes of binding quantification.

2.2. Mitigation of Non-Specific Adsorption

Non-specific adsorption of background proteins is a major concern when testing for biomarkers in clinically relevant samples. Serum albumin constitutes about 50% of the blood serum proteins, and is, therefore, an appropriate "fouling" protein to serve as the background against which SA may be detected. **Figure 4**A shows the adsorption of bovine serum albumin (BSA) on graphite after washing (corresponding sensogram in Figure 4D). The protein is present on the entire surface and agglomerates into fibers as the result of drying. The sensogram shows robust detection of binding at 50 ng/ml, followed by increased binding with overall resistance shift of almost 200kΩ at 10 μg/ml, probably due to the formation of a multi-layer film. In order to prevent non-specific adsorption of BSA, we employed the SS-GrBP5 mutant (Table 1), identified in an earlier study as a mutation of GrBP5 that is capable of assembling into ordered monolayers and presenting hydrophilic chemistry on the surface (e.g., 36° contact angle at 100% coverage).[52] Such a contact angle value is similar to those achieved in literature by self-assembled monolayer polyethylene glycol anti-fouling systems (about 32°).[43,55,56] The contact angle value has been strongly linked to anti-fouling properties in a variety of systems.[57] We, therefore, hypothesized that our self-assembled peptide monolayers, which are dense and exhibit similar contact angles, would also be anti-fouling. To test this hypothesis, we assembled SS-GrBP5 peptide (Figure 4B) on the sensor surface, and introduced BSA to the system (Figures 4C and E). The binding of BSA was significantly impaired by the SS-GrBP5 mutant, resulting in no detectable binding at less than 10 μg/ml concentrations of BSA. The AFM image of the surface after incubation with 10 μg/ml BSA for 90 minutes (Figure 4C) displays a small amount

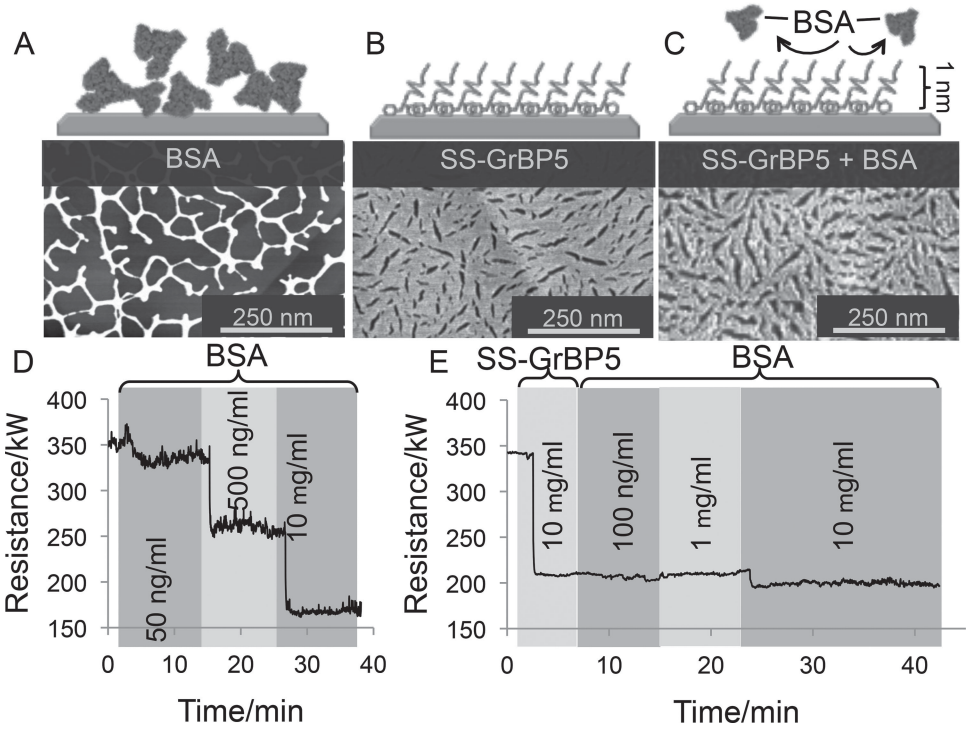

Figure 4. A) AFM image and schematics of 10 mg/ml BSA adsorption to bare graphite; B) AFM image and schematics of 10 mg/ml SS-GrBP5 on graphite; C) AFM image and schematics of 10 mg/ml BSA adsorption blocked by SS-GrBP5-functionalized graphite; D) Sensogram showing the effect of sequentially increasing concentrations of BSA added to bare sensor; E) Sensogram of sequentially increasing concentrations of BSA added to SS-GrBP5 functionalized sensor.

NANO MICRO small

of protein present sparsely on the surface and very low degradation of the underlying peptide monolayer. The added stability, as compared to the bio-GrBP5 mutant, is likely the result of the more amphiphilic nature of the SS-GrBP5 monolayer among the two peptides, which remains robustly oriented between the hydrophobic graphite and water. As a control experiment, we introduced BSA to a monolayer of bio-GrBP5 (Figures S2). The sensogram shows significant, nonspecific, binding of BSA.

2.3. Multi-Functional Surfaces Through Peptide Co-Assembly

By combining the passivating SS-GrBP5 with the biotinilated probe peptide, bio-GrBP5, we created a sensor capable of selective detection of streptavidin in a bovine serum albumin solution. A mixed peptide monolayer with optimized ratio (see below), i.e., consisting of 25% bio-GrBP5 and 75% SS-GrBP5, was formed in a single step from a solution with an overall peptide concentration of 10 µg/ml. The AFM of the resulting monolayer (**Figure 5**A) shows that the peptides self-assembled into a dense ordered structure with no discernible segregation, leading to the conclusion that the peptides are completely miscible in each other and, therefore, they do not hinder each other's binding and self-assembly characteristics on the common graphene substrate surface.

Guided by the results in Figure 4, we introduced 5 µg/ml BSA to the sensor and detected no binding (Figure 5C). We then introduced sequentially increasing concentrations of SA to the sensor, while maintaining the levels of BSA in the solution, and were able to reliably detect streptavidin at 100 ng/ml, although some signal was present at even lower concentrations (Figure 5C). The AFM image of the graphite surface at the final conditions (Figure 5B) showed less coverage by SA than the biotin-only surface (Figure 3B). The overall stability of the bio-GrBP5 appears to have been improved by co-assembly with SS-GrBP5, displaying very high coverage and density. The passivating peptide SS-GrBP5 also seems to retain its anti-fouling function despite a 25% reduction in coverage, owing to the fact that the overall order of the monolayer is maintained by the co-self-assembling sequence of bio-GrBP5.

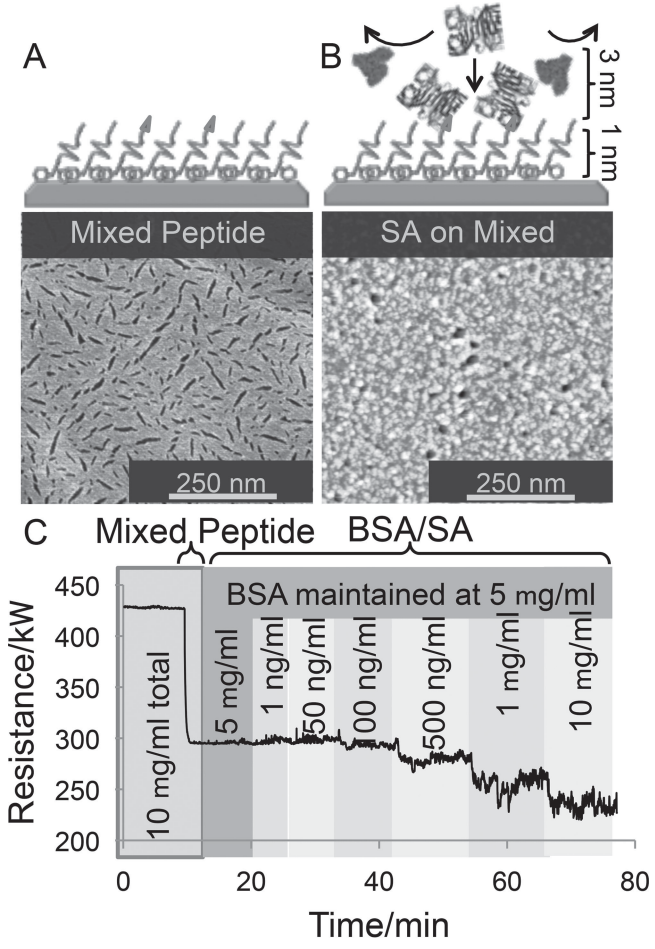

Figure 5. A) AFM image and schematics of mixed peptide monolayer on graphite; B) AFM image and schematics of selective detection of streptavidin against a BSA background; C) The corresponding sensogram of (B), where 25% bio-GrBP5, 75% ss-GrBP5 peptide mixture is introduced first, followed by BSA, which shows no binding, and finally, streptavidin, which is captured selectively.

2.4. Critical SS-GrBP5 Coverage Determination

To optimize the number of probe-bearing peptides in the mixed peptide monolayer we determined the minimum coverage percentage of SS-GrBP5 in the mixed monolayer necessary to maintain the anti-fouling properties of the substrate overall, while maintaining the sensory characteristics. This was accomplished by measuring the K_d of BSA adhering to the sensor as a function of fraction of probe peptide bio-GrBP5 within the SS-GrBP5 mixed monolayer. The dissociation constant K_d was calculated from the shifts in signal in response to increasing concentration of analyte, which was then fitted with the Langmuir equation:

$$\varphi = \varphi_{max} \frac{K_{eq}[C]}{1 + K_{eq}[C]} \quad (1)$$

where ϕ is the amount analyte adsorbed on the surface, φ_{max} is the maximum amount analyte that could be adsorbed on the surface, K_{eq} is the inverse of the K_d, and $[C]$ is the concentration of analyte. It is important to note that, based on this equation, if the available binding sites on the surface are limited, and actual ϕ_{max} is smaller than the equilibrium coverage at a high analyte concentration, the K_{eq} will appear larger (K_d smaller) than it actually is. We refer to this quantity as "apparent K_d".

In addition to the aforementioned probe peptide, we created a second biotin-functionalized peptide, bio-SS-GrBP5 (Table 1), to test the effect of the extra linker on the display of the probe within the mixed monolayer, and its ease of accessibility by the target molecule. To accomplish this task, we first performed contact angle measurements on mixed monolayers at maximum coverage in various ratios of the probe peptides with SS-GrBP5 (**Figure 6**A). The cosines of the resulting contact angles exhibit a linear correlation with the fraction coverage, which is consistent with the Cassie's

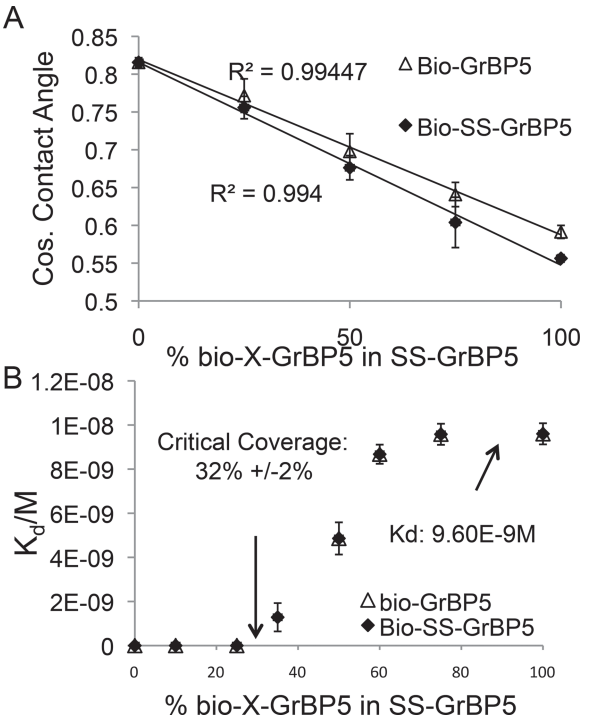

Figure 6. A) Plot of the cosine of the contact angles, showing linear correlation with the relative concentration of the peptide mixture; B) Plot of apparent K_d values as a function of Bio-GrBP5 and Bio-SS-GrBP5 in SS-GrBP%, demonstrating the critical coverage of about 34% (arrow).

Law,[58] indicating that the peptides are, again, fully miscible and are distributed evenly on the surface. Example contact angle measurements are given in Figure S3. The apparent K_d values, shown in Figure 6B, exhibit a transition between no binding and 9.5×10^{-9} M. The transition in apparent K_d values occurs probably because there are insufficiently available binding sites on the surface to reach the equilibrium. The linear extrapolation of the transition region indicates that the critical coverage is 32% ±2% of bio- or bio-SS-GrBP5 in the mixed monolayer, meaning ratios of 2:1 probe-peptide to passivating-peptide are viable. No difference in critical coverage was observed between bio-GrBP5 and bio-SS-GrBP5 mixed monolayers, indicating that the resistance to non-specific adsorption is imparted by the SS-GrBP5 component, independent of the probe-peptide sequence.

2.5. Optimization of Probe Display and Biotin-Streptavidin K_d Measurements

The accessibility of the probe can be a critical factor in biosensor functionalization. To test this crucial function of the displayed biotin in our peptide conjugate system and, at the same time, optimize its affinity for binding, we carried out a series of measurements to determine the apparent K_d values of streptavidin-biotin interactions using both bio-GrBP5 and bio-SS-GrBP5 mixed monolayers with the passivating peptide. We hypothesized that inserting the SS linker into the probe peptide would increase the accessibility of biotin and decrease the K_d of the interaction. The summary of these

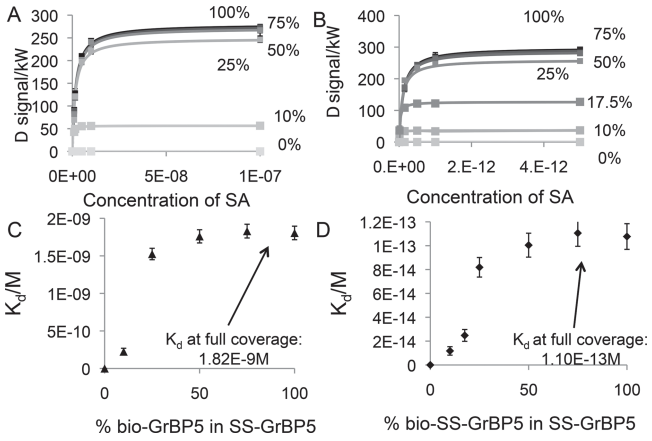

Figure 7. A, B) Change in sensor signal with respect to concentration at different ratios of bio-GrBP5 and bio-SS-GrBP5 to SS-BrBP5 respectively, with corresponding Langmuir fits; C, D) Plots of apparent K_d values of biotin-streptavidin interactions at different ratios of bio-GrBP5 and bio-SS-GrBP5 to SS-BrBP5, respectively.

experiments is given in **Figure 7**. By optimizing the concentration range for our experiments, we again observed a transition of apparent K_d values from no binding to a stable value, corresponding to the low availability of binding sites at low probe coverages. By linearly extrapolating the transition region of the K_d plots (Figure 7C and D) we arrive at a value of approximately 7%, which represents the quantity of inactive (unavailable) probes on the surface.

The equilibrium K_d values obtained via bio-GrBP5 (1.82×10^{-9} M) vary significantly from those obtained via bio-SS-GrBP5 (1.10×10^{-13} M). This is consistent with our hypothesis that the probe entity must be displayed above the surrounding passivating SS-GrBP5 monolayer for accurate detection. The value we obtained from the bio-SS-GrBP5-based system correlates well with the established literature values (5×10^{-14} M).[59]

The sensor devices used in this study were restored and reused. We observed some sensor degradation over the course of about 12 experiments, with the noise levels increasing from near 2k Ω to about 10 kΩ. It appears, however, that the sensitivity of the device is not significantly affected between trials, meaning that it can be reused to produce comparable data repeatedly several times. The initial signal from the device varied in water by approximately 40 kΩ, with standard deviation of about 22 kΩ. This is a significant feature for practical application of graphene-based sensors in terms of their reuse, and represents another advantage of peptide functionalization over covalent approaches. The details of the reuse procedure are given in Section 4 (Experimental).

3. Conclusions

In this study, we demonstrated a system for simultaneous passivation and functionalization of the graphene field effect transistor using modular graphite-binding peptides, based on the engineered dodecapeptide GrBP5, which allows for selective detection of streptavidin against a serum albumin background

NANO MICRO small

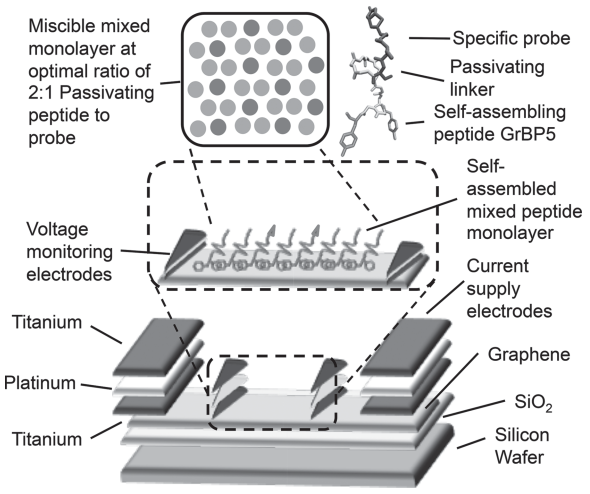

Figure 8. Schematics of the optimized self-assembled peptide functionalized graphene FET bio-sensor.

(**Figure 8**). The system developed can be extended to other sensor architectures, and different single layer materials systems, such as the semi-conducting MoS_2 or WS_2, which can be enabled either through rational mutation of the GrBP5-WT peptide, or through discovery of new peptides specific to these materials. The novel biosensors based on peptide-2D material conjugation opens up a new area in biomolecular detection, not only through electrical signals but also, potentially, through optical and magnetic signals, depending on the physical characteristics (semiconducting, dielectric, etc.) of the 2D material, the interaction of the target biomolecule with the peptide-displayed probe, and the appropriate mode of detection, i.e., electrical, photonic, or magnetic. Our ability to control the functional biomolecular groups displayed by the peptide monolayers as well as the possibility of creating mixed monolayers for controlling the preparation of the sensor surface allow for the construction of multi-functional sensors capable of selective detection of multiple probes in a complex environment. Self-assembled peptides offer unique opportunities for biosensor functionalization, including biocompatibility, non-covalent binding, the ease of fusion with biological probes, as well as a high degree of control over assembly and surface coverage. Based on a variety of short peptidic probes that have been identified for many disease biomarkers, through phage and cell-surface display,[60] the next step for this novel technology would be to create a diagnosis and monitoring system via the formation of fusion proteins (i.e., multifunctional biomolecular constructs) through molecular-genetics based techniques. Furthermore, the peptide-enabled gFET is not limited to clinical applications. Specific ligand receptor interactions are of critical importance to all areas of molecular biology and biotechnology. By upgrading and optimizing the gFET described herein further to include a flow configuration, for example, it would be possible to build a selective biosensor to study the kinetics of various specific ligand-receptor pairs. More broadly, the presented study adds another significant tool to the peptide-based bio-nanotechnology toolkit, taking advantage of molecular biomimetic ways of rationally connecting biomolecular and 2D single atomic layer materials at the nano-scale.

4. Experimental Section

Sensor construction: Graphene samples were prepared by exfoliation method[24] on silica wafers which were pre-treated with acidic piranha solution (75% sulfuric acid, 25% hydrogen peroxide). Orientation markers were made via indium micro-soldering,[61] and a PMMA coating was applied to the wafer by spin-coating 5% PMMA solution for 1 min at 1000 RPM. The electrode patterns (Figure 2B) were made via electron beam lithography on JOEL 7000 SEM (JOEL Ltd., Japan). The pattern was developed and then extended by hand to lengthen the electrodes. The electrodes were made by sputtering 2nm of titanium as adhesion layer, followed by 46 nm of platinum, and 2 nm of titanium as insulating layer using Gatan Precision Etching Coating System Model 682 (Gatan Inc., USA). The PMMA was removed in boiling acetone, and the device annealed in a tube furnace under a 60% argon/40% hydrogen atmosphere at 450 °C for 1 hour. The terminals of indium solder were added at the ends of the electrodes. The contacts were current-annealed under nitrogen atmosphere by cycling currents of up to 1 mA at up to 60 volts through the device using Agilent U2722A USB Modular Source Measure Unit (Agilent. USA), until the resistance of the device remained constant between cycles. The devices were re-cleaned between experiments by boiling in acetone for 1 hour, followed by current-annealing.

Peptides and Proteins: The peptides were produced by solid-state synthesis using a CSBio 336s automated peptide synthesizer (CSBio, USA) on Wang resin via *Fmoc* chemistry and HBTU activation. The crude peptides were purified by reverse phase high performance liquid chromatography to >98% purity (Gemini 10 µm C18 110A column). The purified peptides were verified by mass spectroscopy (MS) using a MALDI-TOF mass spectrometer (Bruker Daltonics Inc., USA). The amino acid sequences and the physiochemical properties of the peptides used in the study are shown in Table 1. HPLC and MS sensograms are presented in the supporting information Figure S4. Streptavidin and bovine serum albumin were purchased from Sigma-Aldrich, USA, and used as received. All of the solutions were prepared with de-ionized water.

Sensor Measurement: The device was connected to the Agilent U2722A USB Modular Source Measure Unit (Agilent, USA) in a four probe configuration, with current (I_{sd}) kept constant at 0.1 µA between R1 and R2 terminals, and voltage (V_{sd}) measured between R3 and R4 terminals (Figure 2C). A 20 µl drop of water was placed on the sensor and the resistance was allowed to equilibrate. The device was maintained in a hydration chamber at 100% humidity to prevent evaporation. Analyte was added to the static drop on the sensor in the appropriate concentrations, using a micropipette so that the total volume of the drop never exceeded 35 µl. As each subsequent analyte is added, the previously used analytes have remained in the test solution. Data was collected from two distinct devices and each experiment was reproduced at least once.

Atomic Force Microscopy: To complement the biosensor results, certain states of each experiment were reproduced on highly-oriented pyrolytic graphite (HOPG) and imaged by atomic force microscopy (AFM). The peptide solutions, at concentrations identical to those used for sensing experiments, were placed on HOPG and allowed to bind for amounts of time (10–90 minutes) similar to those used for graphene. The samples were washed by dilution, dried and immediately imaged using a Digital Instruments

Nanoscope-IIIa Multimode AFM (Veeco, USA) under tapping mode. The images were taken in at least 3 different areas of the sample.

Supporting Information

Supporting Information is available from the Wiley Online Library or from the author.

Acknowledgements

This research was supported by NSF-BioMaterials (DMR-0706655) and MRSEC program (DMR-0520567) at GEMSEC, Genetically Engineered Materials Science and Engineering Center, University of Washington. DK and CG were additionally supported by the NCI Training Grant T32CA138312 and YH by JST PRESTO program (Japan). We thank M. Hnilova and C. R. So (both UW) for helpful discussions. The work was carried out GEMSEC-SECF, a member of Materials Facilities Network of MRSEC. Research reported in this publication was supported by the National Cancer Institute of the National Institutes of Health under award number RO1CA115513, P30CA15704, UO1CA152756, U54CA143862, and P01CA077852, (WMG). The content is solely the responsibility of the authors, and does not necessarily represent the official views of the National Institutes of Health. Support for these studies was also provided by a Burroughs Wellcome Fund Translational Research Award for Clinician Scientist (WMG).

[1] R. S. Yalow, S. A. Berson, *J. Clin. Invest.* **1960**, *39*, 7, 1157–1175.
[2] J. A. Ludwig, J. N. Weinstein, *Nat. Rev. Cancer* **2005**, *5*, 11, 845–856.
[3] H. Vaisocherova, W. Yang, Z. Zhang, Z. Q. Cao, G. Cheng, M. Piliarik, J. Homola, S. Y. Jiang, *Anal. Chem.* **2008**, *80*, *20*, 7894–7901.
[4] S. F. Chou, W. L. Hsu, J. M. Hwang, C. Y. Chen, *Biosens. & Bioelectron.* **2004**, *19*, 9, 999–1005.
[5] C. Di Natale, A. Macagnano, E. Martinelli, R. Paolesse, G. D'Arcangelo, C. Roscioni, A. Finazzi-Agro, A. D'Amico, *Biosens. & Bioelectron.* **2003**, *18*, 10, 1209–1218.
[6] X. Yu, B. Munge, V. Patel, G. Jensen, A. Bhirde, J. D. Gong, S. N. Kim, J. Gillespie, J. S. Gutkind, F. Papadimitrakopoulos, J. F. Rusling, *J. Am. Chem. Soc.* **2006**, *128*, 34, 11199–11205.
[7] V. Mani, B. V. Chikkaveeraiah, V. Patel, J. S. Gutkind, J. F. Rusling, *ACS Nano* **2009**, *3*, 3, 585–594.
[8] X. Liu, Q. Dai, L. Austin, J. Coutts, G. Knowles, J. H. Zou, H. Chen, Q. Huo, *J. Am. Chem. Soc.* **2008**, *130*, 9, 2780–2782.
[9] G. D. Liu, Y. Y. Lin, J. Wang, H. Wu, C. M. Wai, Y. H. Lin, *Anal. Chem.* **2007**, *79*, 20, 7644–7653.
[10] M. Curreli, R. Zhang, F. N. Ishikawa, H. K. Chang, R. J. Cote, C. Zhou, M. E. Thompson, *IEEE T. Nanotechnol.* **2008**, *7*, 6, 651–667.
[11] M. M. Alam, J. Wang, Y. Y. Guo, S. P. Lee, H. R. Tseng, *J. Phys. Chem. B* **2005**, *109*, 26, 12777–12784.
[12] W. R. Yang, K. R. Ratinac, S. P. Ringer, P. Thordarson, J. J. Gooding, F. Braet, *Angew. Chem.* **2010**, *49*, 12, 2114–2138.
[13] H. G. Sudibya, J. M. Ma, X. C. Dong, S. Ng, L. J. Li, X. W. Liu, P. Chen, *Angew. Chem.* **2009**, *48*, 15, 2723–2726.
[14] S. Liu, X. F. Guo, *Npg Asia Mater.* **2012**, *4*, 1–10.
[15] X. C. Dong, Y. M. Shi, W. Huang, P. Chen, L. J. Li, *Adv. Mater.* **2010**, *22*, 14, 1649–1653.
[16] Y. Ohno, K. Maehashi, K. Matsumoto, *Biosens. Bioelectron.* **2010**, *26*, 4, 1727–1730.
[17] N. Mohanty, V. Berry, *Nano Lett.* **2008**, *8*, 12, 4469–4476.
[18] Y. Ohno, K. Maehashi, K. Matsumoto, *J. Am. Chem. Soc.* **2010**, *132*, 51, 18012–18013.
[19] R. Stine, J. T. Robinson, P. E. Sheehan, C. R. Tamanaha, *Adv. Mater.* **2010**, *22*, 46, 5297–5300.
[20] T. Someya, J. Small, P. Kim, C. Nuckolls, J. T. Yardley, *Nano Lett.* **2003**, *3*, 7, 877–881.
[21] T. R. Page, Y. Hayamizu, C. R. So, M. Sarikaya, *Biosens. Bioelectron.* **2012**, *33*, 1, 304–308.
[22] B. Zhang, Q. Li, T. H. Cui, *Biosens. Bioelectron.* **2012**, *31*, 1, 105–109.
[23] A. H. Castro Neto, F. Guinea, N. M. R. Peres, K. S. Novoselov, A. K. Geim, *Rev. Mod. Phys.* **2009**, *81*, 1, 109–162.
[24] K. S. Novoselov, A. K. Geim, S. V. Morozov, D. Jiang, Y. Zhang, S. V. Dubonos, I. V. Grigorieva, A. A. Firsov, *Science* **2004**, *306*, 5696, 666–669.
[25] A. A. Balandin, S. Ghosh, W. Z. Bao, I. Calizo, D. Teweldebrhan, F. Miao, C. N. Lau, *Nano Lett.* **2008**, *8*, 3, 902–907.
[26] K. R. Ratinac, W. R. Yang, J. J. Gooding, P. Thordarson, F. Braet, *Electroanalysis* **2011**, *23*, 4, 803–826.
[27] A. K. M. Newaz, Y. S. Puzyrev, B. Wang, S. T. Pantelides, K. I. Bolotin, *Nat. Commun.* **2012**, *3*, 6.
[28] D. Li, M. B. Muller, S. Gilje, R. B. Kaner, G. G. Wallace, *Nat. Nanotechnol.* **2008**, *3*, 2, 101–105.
[29] S. Niyogi, E. Bekyarova, M. E. Itkis, J. L. McWilliams, M. A. Hamon, R. C. Haddon, *J. Am. Chem. Soc.* **2006**, *128*, 24, 7720–7721.
[30] T. Kuila, S. Bose, A. K. Mishra, P. Khanra, N. H. Kim, J. H. Lee, *Progress in Materials Science* **2012**, *57*, 7, 1061–1105.
[31] E. Y. Choi, T. H. Han, J. H. Hong, J. E. Kim, S. H. Lee, H. W. Kim, S. O. Kim, *J. Mater. Chem.* **2010**, *20*, 10, 1907–1912.
[32] A. Ghosh, K. V. Rao, R. Voggu, S. J. George, *Chem. Phys. Lett.* **2010**, *488*, 4–6, 198–201.
[33] C. Chung, Y.-K. Kim, D. Shin, S.-R. Ryoo, B. H. Hong, D.-H. Min, *Accounts of Chemical Research* **2013**, *46*, 10, 2211–2224.
[34] S. Mao, G. Lu, K. Yu, Z. Bo, J. Chen, *Adv. Mater.* **2010**, *22*, 32, 3521.
[35] J. B. Chang, S. Mao, Y. Zhang, S. M. Cui, D. A. Steeber, J. H. Chen, *Biosensors & Bioelectronics* **2013**, *42*, 186–192.
[36] K. Shiba, *Curr. Opin. Biotechnol.* **2010**, *21*, 4, 412–425.
[37] C. Tamerler, D. Khatayevich, M. Gungormus, T. Kacar, E. E. Oren, M. Hnilova, M. Sarikaya, *Biopolymers* **2010**, *94*, 1, 78–94.
[38] B. R. Peelle, E. M. Krauland, K. D. Wittrup, A. M. Belcher, *Langmuir* **2005**, *21*, 15, 6929–6933.
[39] M. Sarikaya, C. Tamerler, A. K. Y. Jen, K. Schulten, F. Baneyx, *Nat. Mater.* **2003**, *2*, 9, 577–585.
[40] J. H. Wei, T. Kacar, C. Tamerler, M. Sarikaya, D. S. Ginger, *Small* **2009**, *5*, 6, 689–693.
[41] M. Hnilova, E. E. Oren, U. O. S. Seker, B. R. Wilson, S. Collino, J. S. Evans, C. Tamerler, M. Sarikaya, *Langmuir* **2008**, *24*, 21, 12440–12445.
[42] S. R. Meyers, X. J. Khoo, X. Huang, E. B. Walsh, M. W. Grinstaff, D. J. Kenan, *Biomaterials* **2009**, *30*, 3, 277–286.
[43] D. Khatayevich, M. Gungormus, H. Yazici, C. So, S. Cetinel, H. Ma, A. Jen, C. Tamerler, M. Sarikaya, *Acta Biomater.* **2010**, *6*, 12, 4634–4641.
[44] H. Yang, S. Y. Fung, W. Sun, S. Mikkelsen, M. Pritzker, P. Chen, *Biotechnol. Prog.* **2008**, *24*, 4, 964–971.
[45] Y. Cui, S. N. Kim, S. E. Jones, L. L. Wissler, R. R. Naik, M. C. McAlpine, *Nano Lett.* **2010**, *10*, 11, 4559–4565.
[46] Q. H. Wang, M. C. Hersam, *Nat. Chem.* **2009**, *1*, 3, 206–211.
[47] S. N. Kim, Z. F. Kuang, J. M. Slocik, S. E. Jones, Y. Cui, B. L. Farmer, M. C. McAlpine, R. R. Naik, *J. Am. Chem. Soc.* **2011**, *133*, 37, 14480–14483.

[48] D. Kase, J. L. Kulp, M. Yudasaka, J. S. Evans, S. Iijima, K. Shiba, *Langmuir* **2004**, *20*, 20, 8939–8941.
[49] S. M. Tomasio, T. R. Walsh, *J. Phys. Chem. C* **2009**, *113*, 20, 8778–8785.
[50] T. H. Han, W. J. Lee, D. H. Lee, J. E. Kim, E. Y. Choi, S. O. Kim, *Adv. Mater.* **2010**, *22*, 18, 2060–2064.
[51] C. R. So, Y. Hayamizu, H. Yazici, C. Gresswell, D. Khatayevich, C. Tamerler, M. Sarikaya, *ACS Nano* **2012**, *6*, 2, 1648–1656.
[52] D. Khatayevich, C. R. So, Y. Hayamizu, C. Gresswell, M. Sarikaya, *Langmuir* **2012**, *28*, 23, 8589–8593.
[53] F. Schedin, A. K. Geim, S. V. Morozov, E. W. Hill, P. Blake, M. I. Katsnelson, K. S. Novoselov, *Nat. Mater.* **2007**, *6*, *9*, 652–655.
[54] Y. Ohno, K. Maehashi, Y. Yamashiro, K. Matsumoto, *Nano Lett.* **2009**, *9*, 9, 3318–3322.
[55] P. Harder, M. Grunze, R. Dahint, G. M. Whitesides, P. E. Laibinis, *J. Phys. Chem. B* **1998**, *102*, 2, 426–436.
[56] N. Faucheux, R. Schweiss, K. Lutzow, C. Werner, T. Groth, *Biomaterials* **2004**, *25*, 14, 2721–2730.
[57] K. L. Menzies, L. Jones, *Optometry Vision Sci.* **2010**, *87*, 6, 387–399.
[58] A. B. D. Cassie, S. Baxter, *T. Faraday Soc.* **1944**, *40*, 0546–0550.
[59] A. Holmberg, A. Blomstergren, O. Nord, M. Lukacs, J. Lundeberg, M. Uhlen, *Electrophoresis* **2005**, *26*, 3, 501–510.
[60] S. A. Soper, K. Brown, A. Ellington, B. Frazier, G. Garcia-Manero, V. Gau, S. I. Gutman, D. F. Hayes, B. Korte, J. L. Landers, D. Larson, F. Ligler, A. Majumdar, M. Mascini, D. Nolte, Z. Rosenzweig, J. Wang, D. Wilson, *Biosens. Bioelectron.* **2006**, *21*, 10, 1932–1942.
[61] C. O. Girit, A. Zettl, *Appl. Phys. Lett.* **2007**, *91*, 19.

Received: July 17, 2013
Revised: November 16, 2013
Published online: March 26, 2014

